RAPID COMMUNICATIONS

PHYSICAL REVIEW E VOLUME 47, NUMBER 4 APRIL 1993

Laser-induced electron acceleration in a counterpropagating rf field

Liang Feng
Physics Department 2, Fudan University, Shanghai 200433, China

Yu-kun Ho
*Centre of Theoretical Physics, China Center of Advanced Science and Technology (World Laboratory), Beijing, China and Physics Department 2, Fudan University, Shanghai 200433, China**

(Received 11 December 1992)

Laser-driven electron acceleration by means of two counterpropagating waves is investigated, where the comoving field is an intense laser light beam, the other is a rf wave beam. A striking feature of the interaction is the presence of a ponderomotive potential propagating with phase velocity slower than the speed of light, allowing one to achieve wave-particle matching. Electron trajectories in the combined field are derived analytically, following the plane-wave and single-particle approximations. Special attention has been given to analyzing the phase slippage of an electron in the field, and the potential of accelerating electrons by means of this scheme. The results show that a neodymium-doped yttrium aluminum garnet laser beam with wavelength 1.06 μm and electric field intensity 4×10^{10} V/cm is capable of accelerating electrons from 43 to 258 MeV over 0.27 m by using a rf field of wavelength 10.6 cm and an electric field of 10^5 V/cm. The averaged accelerating gradient is 1038 MeV/m.

PACS number(s): 41.75.Fr, 29.17.+w, 41.85.−p, 42.62.Hk

The use of lasers to accelerate electrons is attractive. The accelerating gradient for conventional linacs is about 10^5 V/cm, while powerful focused lasers can produce electric fields as high as 10^{11} V/cm. A wide variety of laser-based accelerator schemes are being explored. Generally, those schemes can be divided into two categories, depending on whether the acceleration takes place in vacuum or in media. The emerged schemes associated with the former are those such as the inverse free-electron laser [1], coupling light either to slow-wave structure near walls [2] or to lens waveguide array [3], as well as many other proposals [4–7]. The second category of laser-based accelerator schemes includes the plasma-beat wave accelerator [8,9] and inverse Čerenkov accelerator [10]. A common feature of the media accelerators is that the accelerating fields propagate with phase velocities less than c, the speed of light in vacuum, owing to the fact that the index of refraction in a medium is larger than 1. This feature could be used to minimize the phase slippage of particles in the accelerating field, permitting the particles to receive more energy from the field. However, there are always troublesome problems in connection with the breakdown of media by intense electric field or the complex features of plasma physics such as instabilities and nonlinearities, which are hard to control. Furthermore, the loaded accelerators are limited by multiple collisions of electrons with media, causing energy loss and beam spreading.

In this Rapid Communication, we discuss an alternative method to produce a longitudinal accelerating potential in vacuum with a phase velocity slower than c. We study the particle dynamics in the combined field of two counterpropagating electromagnetic radiation beams with greatly different frequencies. Emphasis will be put on analyzing the trajectories of electrons in the phase space of the waves and exploring the potential of using this scheme to accelerate electrons.

Figure 1 illustrates the proposed arrangement. The relativistic electron is moving along the z axis, which is also the propagation direction of the intense laser light beam. The rf wave beam propagates in the opposite z direction. For simplicity, we assume that both the waves are monochromatic, circularly polarized plane waves with vector potentials

$$\mathbf{A}_0 = A_0(\hat{\mathbf{x}}\cos\phi + \hat{\mathbf{y}}\sin\phi) \tag{1}$$

and

$$\mathbf{A}_1 = A_1(\hat{\mathbf{x}}\cos\eta + \hat{\mathbf{y}}\sin\eta)\ , \tag{2}$$

where $\phi=\omega_0 t - k_0 z + \phi_0$, $\eta=\omega_1 t + k_1 z$, $[\omega_0, \mathbf{k}_0(0,0,k_0)]$ and $[\omega_1, \mathbf{k}_1(0,0,-k_1)]$ denote the frequencies and wave vectors of the laser and rf field, respectively, and ϕ_0 designates the initial phase of the laser field. The amplitudes of the two potentials, A_0 and A_1, are taken to be constant in the present study. $\hat{\mathbf{x}}$, $\hat{\mathbf{y}}$, and $\hat{\mathbf{z}}$ are the unit vectors along the x, y, and z axes, respectively. The related electric fields and magnetic fields are found by

$$\mathcal{E}_i = -\frac{\partial \mathbf{A}_i}{\partial t} = -\omega_i(\hat{\mathbf{z}}\times\mathbf{A}_i)\ , \tag{3}$$

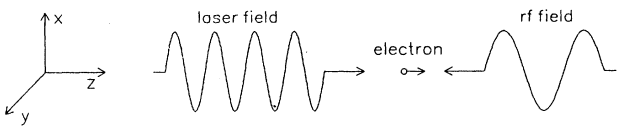

FIG. 1. Configuration for electron acceleration in two counterpropagating electromagnetic waves.

$$\mathcal{B}_i=\nabla\times\mathbf{A}_i=(\mathbf{k}_i\cdot\hat{\mathbf{z}})\mathbf{A}_i,\quad i=0,1\ . \tag{4}$$

Assuming that the energy transferred to the electrons is not strong enough to affect the fields, then the dynamic equations of an electron with rest mass m_0 and charge q are given by

$$\frac{d\mathbf{P}_\perp}{dt}=-q\frac{d(\mathbf{A}_0+\mathbf{A}_1)}{dt}\ , \tag{5}$$

$$\frac{d\mathbf{P}_z}{dt}=q\mathbf{V}_\perp\times(\mathcal{B}_0+\mathcal{B}_1)\ , \tag{6}$$

$$mc^2\frac{d\gamma}{dt}=q(\mathcal{E}_0+\mathcal{E}_1)\cdot\mathbf{V}_\perp\ . \tag{7}$$

The subscript $\perp$ denotes the component in the transverse direction, $\mathbf{P}$ is the electron momentum, and $\mathbf{V}$ is the velocity.

From Eq. (5), we can easily obtain an integral of motion

$$\mathbf{P}_\perp+q(\mathbf{A}_0+\mathbf{A}_1)=\mathcal{K}_1\ ; \tag{8}$$

$\mathcal{K}_1$ is a constant determined from the initial condition. For simplicity and without losing any physical ingredient, we assume $\mathcal{K}_1=0$, which means that we neglect the transverse velocity of the electron before it enters the field. Thus one has

$$\mathbf{V}_\perp=-\frac{q}{m_0\gamma}(\mathbf{A}_0+\mathbf{A}_1)\ . \tag{9}$$

By inserting Eq. (9) into (6) and (7), it yields

$$\frac{d\gamma}{dt}=\left[\frac{qA_0}{m_0c}\right]\left[\frac{qA_1}{m_0c}\right]\frac{1}{\gamma}(\omega_0-\omega_1)\sin\psi\ , \tag{10}$$

$$\frac{d\beta_z}{dt}=\left[\frac{qA_0}{m_0c}\right]\left[\frac{qA_1}{m_0c}\right]\frac{1}{\gamma^2}[\omega_0(1-\beta_z)+\omega_1(1+\beta_z)]\sin\psi\ , \tag{11}$$

where γ is the Lorentz factor, $\beta_z=V_z/c$, and $\psi=(\omega_0-\omega_1)t-(k_0+k_1)z$ is the particle phase in the field. Equation (10) illustrates that the electron moves in a so-called ponderomotive potential with phase velocity given by

$$V_\psi=\frac{\omega_0-\omega_1}{\omega_0+\omega_1}c\ . \tag{12}$$

The fact that the phase velocity is slower than c and changeable by adjusting the ratio ω_1/ω_0 is a striking feature of this scheme, since it could minimize the slippage of the particle in the field and, consequently, cause synchronous particle-wave coupling. Typically, we take the wavelengths of the two waves to be $\lambda_0=1.06$ μm and $\lambda_1=10.6$ cm, respectively. Then the phase velocity from Eq. (12) is $\beta_\psi=V_\psi/c=0.999\,98$. We note that the ponderomotive potential arises from the nonlinear interaction of the two waves where the transverse electric field of one wave gives the particle transverse velocity that causes longitudinal acceleration through the $\mathbf{V}\times\mathcal{B}$ force of another wave. The equation describing the phase slippage of the particle in the field is

$$\frac{d\psi}{dt}=\frac{\omega_0}{2}(1+\beta_z)(\beta_z-\beta_\psi)\ . \tag{13}$$

Thus if $\beta_z<\beta_\psi$, one gets $d\psi/dt<0$, the particle slips behind the potential propagation, and vice versa.

Next, we study the dynamic characteristics of electrons moving in the field by solving the set of equations (10)–(13). From Eqs. (10) and (11), one can find another integral of motion

$$\mathcal{K}_2=\gamma\left[\left[1+\frac{\omega_1}{\omega_0}\right]-\left[1-\frac{\omega_1}{\omega_0}\right]\beta_z\right]\ . \tag{14}$$

$\mathcal{K}_2$ is a constant of motion determined by the initial conditions. By taking account of the fact that

$$\gamma^{-2}=1-\beta_z^2-\frac{q^2}{\gamma^2m_0^2c^2}(\mathbf{A}_0+\mathbf{A}_1)^2\ , \tag{15}$$

Eq. (11) becomes

$$\left[(1-\beta_z)+\frac{\omega_1}{\omega_0}(1+\beta_z)\right]\frac{1}{(1-\beta_z^2)^{1/2}}=\frac{\mathcal{K}_2}{\left[1+\left[\frac{q}{m_0c}\right]^2(A_0^2+A_1^2+2A_0A_1\cos\psi)\right]^{1/2}}\ . \tag{16}$$

By setting

$$\frac{\mathcal{K}_2}{\left[1+\left[\frac{q}{m_0c}\right]^2(A_0^2+A_1^2+2A_0A_1\cos\psi)\right]^{1/2}}=\alpha(\psi)\ , \tag{17}$$

which is a periodic function of ψ, the solution of Eq. (16) provides

$$\beta_z=-\frac{1-\left[\frac{\omega_1}{\omega_0}\right]^2\pm\alpha(\psi)\left[[\alpha(\psi)]^2-4\left[\frac{\omega_1}{\omega_0}\right]\right]^{1/2}}{[\alpha(\psi)]^2+\left[1-\left[\frac{\omega_1}{\omega_0}\right]\right]^2}\ . \tag{18}$$

Figure 2 shows the predicted trajectories of electrons in the P_z-ψ phase plane with representive field parameters $\omega_1/\omega_0=10^{-5}$, $E_0=4\times10^{10}$ V/cm, and $E_1=1\times10^5$ V/cm. We note from Eqs. (10) and (11) that the phase space $\psi=0-\pi$ is the accelerating part, whereas $\psi=\pi-2\pi$ is the decelerating part. The whole P_z-ψ plane can be divided into three regions delimited by the dot-dashed curve in the figure. Once a particle locates in one of the regions, it remains so. There is no trajectory intersecting the region boundaries. For instance, consider an electron moving in the $\mathcal{D}_1$ ($\mathcal{D}_3$) region. The longitudinal velocity remains faster (slower) than the phase velocity V_ψ all along. The phase of the electron continues to increase (decrease) when the electron travels in the field, as depicted by the solid line a (c) in Fig. 2. From Eq. (18), this requirement corresponds to the condition that

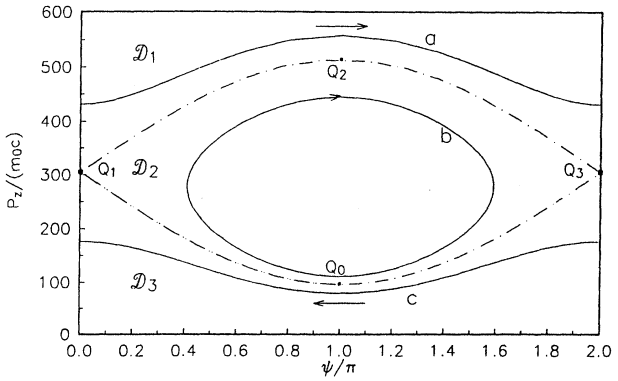

FIG. 2. Phase-space plots for electron trajectories in the configuration shown in Fig. 1. The adopted field parameters are $\lambda_0=1.06$ μm, $\lambda_1=10.6$ cm, $E_0=4\times10^{10}$ V/cm, and $E_1=10^5$ V/cm. The whole phase plane is divided into three regions $\mathcal{D}_1$, $\mathcal{D}_2$, and $\mathcal{D}_3$ bounded by the dot-dashed curve. The solid lines *a*, *b*, and *c* are representive electron trajectories in the three regions, respectively. See text for the details.

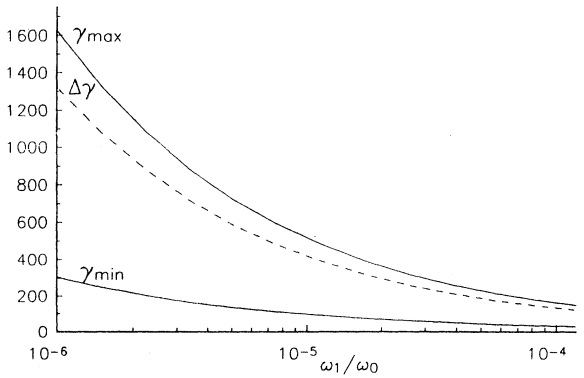

FIG. 3. γ_{max} and γ_{min} correspond to the energies for electrons at the phase-space points Q_0 and Q_2 in Fig. 2, respectively. $\Delta\gamma=\gamma_{max}-\gamma_{min}$ is the maximum acceleration for electrons trapped in the limited ψ range (the region $\mathcal{D}_2$ in Fig. 2). The plot shows γ_{max}, γ_{min}, and $\Delta\gamma$ as a function of ω_1/ω_0. The radiation field parameters are taken to be $-qA_0/(m_0c)=1.32$ and $-qA_1/(m_0c)=0.33$.

$$[\alpha(\psi)]^2-4\left[\frac{\omega_1}{\omega_0}\right]>0 \tag{19}$$

should be held for all values of ψ. Since

$$[\alpha(\psi)]^2-4\left[\frac{\omega_1}{\omega_0}\right]=\frac{4}{(1+\beta_\psi)^2(1-\beta_z^2)}(\beta_\psi-\beta_z)^2\ , \tag{20}$$

thus Eq. (19) is equivalent to $\beta_z>\beta_\psi$ or $\beta_z<\beta_\psi$ for all ψ values. Of great interest, the trajectory for a particle in the region $\mathcal{D}_2$ is confined in a limited ψ space less than 2π, as shown by the solid closed phase curve *b* in Fig. 2. Physically, this corresponds to the situation where the electron travels nearly in phase with the wave and is trapped in one of the wave valleys. Its longitudinal velocity oscillates around V_ψ. The dot-dashed curve in Fig. 2 can be regarded as the limit of the trapped trajectories. Now let us consider an example of an electron trajectory in this region. Postulate that the electron is injected at the point Q_0 in the P_z-ψ plane with $\psi=\pi$ and $\gamma=\gamma_{min}$. Since the initial velocity component $\beta_z<\beta_\psi$, the electron will slip behind the potential and travel in the accelerating region. After passing through the point Q_1 where $\psi\sim0^+$ and $\beta_z\sim\beta_\psi$, the electron will slip ahead of the potential and still stay in the accelerating region. The electron energy will continue to increase until it arrives at Q_2, where $\psi=\pi$ and $\gamma=\gamma_{max}$. From then on, the electron enters the decelerating region for a total of 2π phase slippage until it returns to the original point Q_0. The amplitude of the electron oscillating in the ψ axis is determined by

$$[\alpha(\psi)]^2-4\left[\frac{\omega_1}{\omega_0}\right]=0\ . \tag{21}$$

Obviously, electrons of trajectories in the region $\mathcal{D}_2$ are accelerated more effectively by the field due to $V_z\sim V_\psi$ and twice passing successively through the acceleration region. With the same parameters as in Fig. 2, an electron in the region $\mathcal{D}_2$ could be accelerated, to the maximum extent, from $\gamma_{min}=85$ to $\gamma_{max}=515$ over a distance $k_0\Delta z=1.3\times10^6$. The transverse undulating amplitude is about 70 μm. The average accelerating gradient is 1038 MeV/m. We present a plot in Fig. 3 showing γ_{max}, γ_{min}, and $\Delta\gamma$ as a function of ψ under the conditions $-qA_0/(m_0c)=1.32$, $-qA_1/(m_0c)=0.33$, $\lambda_0=1.06$ μm, $\lambda_1=10.6$ cm.

Few additional comments may be made concerning this scheme. It can be seen from Eq. (10) and Fig. 2 that the particle energy, regardless of the regimes in which it travels, depends sinusoidally on the phase. The electron will undergo alternatively acceleration and deceleration, if it moves in free space over an unlimited interaction length. Hence the chief problem of utilizing this scheme for a linac is to inject and remove the electron at the correct positions. There have been a number of proposals for this difficult task [3,11], and we plan to specifically address this problem elsewhere. Synchrotron-radiation loss resulting from the transverse electron motion will become severe above 100 GeV. This mechanism is negligible for the considered parameter values.

In summary, we have studied the dynamics of relativistic electrons in the combined field of two counterpropagating radiation beams. The resultant ponderomotive potential with phase velocity slower than *c* is a nonlinear effect of the particle coupling with waves. This interaction may be viewed as a stimulated Compton effect. Alternatively, this configuration is a type of the inverse free-electron lasers where the conventional magnetostatic field is replaced by using a larger amplitude electromagnetic wave to induce undulating motion. This motion allows electrons to receive or give energy to the laser field. There are many questions left open for further discussion. However, it seems worth it to study this scheme as a potential linac.

The authors are grateful for stimulating and helpful interactions with Professor M. O. Scully and Dr. E. T. Cheng. This work is partly supported by the Natural Science Foundation of China.

*Address for correspondence.

[1] W. Colson and S. Ride, Appl. Phys. **20**, 61 (1979).
[2] T. C. Katsouleas, SPIE **664**, 2 (1986), and references therein.
[3] M. O. Scully and M. S. Zubairy, Phys. Rev. A **44**, 2656 (1991).
[4] A. A. Chernikov and G. Schmidt, Phys. Rev. Lett. **68**, 1507 (1992).
[5] M. S. Hussein and M. P. Pato, Phys. Rev. Lett. **68**, 1136 (1992).
[6] L. Cicchitelli, H. Hora, and R. Postle, Phys. Rev. A **41**, 3727 (1990).
[7] A. Loeb and L. Friedland, Phys. Rev. A **33**, 1828 (1986).
[8] R. H. Pantell and T. I. Smith, Appl. Phys. Lett. **51**, 753 (1982).
[9] T. Katsouleas and J. M. Dawson, Phys. Rev. Lett. **51**, 392 (1983).
[10] R. Sugihara, Jpn. J. Appl. Phys. **30**, 76 (1991).
[11] J. A. Edighoffer and R. H. Pantell, J. Appl. Phys. **50**, 6120 (1979).